HHS Public Access

Author manuscript

Trends Immunol. Author manuscript; available in PMC 2021 May 02.

Published in final edited form as:

Trends Immunol. 2021 March ; 42(3): 209–227. doi:10.1016/j.it.2020.12.008.

VISTA: A Mediator of Quiescence and a Promising Target in Cancer Immunotherapy

Long Yuan[1,2], **Jahnavi Tatineni**[2], **Kathleen M. Mahoney**[2,3], **Gordon J. Freeman**[2,*]

[1]Program in Immunology, Harvard Medical School, Boston, MA 02115, USA

[2]Department of Medical Oncology, Dana-Farber Cancer Institute, Harvard Medical School, Boston, MA 02215, USA

[3]Division of Hematology and Oncology, Beth Israel Deaconess Medical Center, Harvard Medical School, Boston, MA 02215, USA

Abstract

V-domain Ig suppressor of T cell activation (VISTA) is a B7 family member that maintains T cell and myeloid quiescence and is a promising target for combination cancer immunotherapy. During inflammatory challenges, VISTA activity reprograms macrophages towards reduced production of proinflammatory cytokines and increased production of interleukin (IL)-10 and other anti-inflammatory mediators. The interaction of VISTA with its ligands is regulated by pH, and the acidic pH ~6.0 in the tumor microenvironment (TME) facilitates VISTA binding to P-selectin glycoprotein ligand 1 (PSGL-1). Targeting intratumoral pH might be a way to reduce the immunoinhibitory activity of the VISTA pathway and enhance antitumor immune responses. We review differences among VISTA therapeutics under development as candidate immunotherapies, focusing on VISTA binding partners and the unique structural features of this interaction.

VISTA: How This B7 Protein Might Transform Cancer Immunotherapy

Immunotherapy has become an established pillar of cancer treatment, in large part owing to the success of blocking the **programmed cell death protein 1 (PD-1)/ programmed death-ligand 1 (PD-L1) immune checkpoint** (see Glossary) pathway. As recent research deepens our understanding of V-domain Ig suppressor of T cell activation (VISTA), the VISTA signaling pathway has increasingly become a promising target for overcoming resistance to current immune checkpoint therapies [1]. Although the development of VISTA

*Correspondence: gordon_freeman@dfci.harvard.edu (G.J. Freeman).

Author Contributions

All authors wrote and edited the manuscript.

Declaration of Interests

G.J.F. has patents/pending royalties on the PD-1/PD-L1 pathway from Roche, Merck MSD, Bristol-Myers-Squibb, Merck KGA, Boehringer-Ingelheim, AstraZeneca, Dako, Leica, Mayo Clinic, and Novartis. G.J.F. has served on advisory boards for Roche, Bristol-Myers-Squibb, Xios, Origimed, Triursus, iTeos, NextPoint, IgM, Jubilant, Trillium, and GV20. G.J.F. has equity in Nextpoint, Triursus, Xios, iTeos, IgM, and GV20. K.M.M. reports research support from Bristol-Myers Squibb. The other authors have no conflicts to declare.

Resources

blocking antibodies has not reached fruition clinically, this review highlights the new features of VISTA that make this pathway particularly attractive for therapeutic development. We discuss (i) VISTA expression on immune cells in the tumor microenvironment (TME), (ii) the biological functions and bidirectional signaling pathways of VISTA in mammalian lymphocytes and myeloid cells, (iii) the structural features of VISTA that contribute to its molecular interactions, (iv) current VISTA monoclonal antibodies (mAbs) that are in clinical development, and (v) the candidate druggable targets that regulate the pH of the TME and which in turn might affect VISTA activity *in vivo*. This review gives a detailed picture of VISTA structure in the context of its binding partners and therapeutic antibodies targeting VISTA.

VISTA Structure

VISTA, also known as PD-1H, B7-H5, Dies1, Gi24, DD1α, and C10orf54, is encoded by the *VSIR* gene in human (*Vsir* in mouse) and has multiple unique features, including its interaction with two receptors that bind to overlapping but distinct sites on the VISTA extracellular domain (ECD) [2–4]. VISTA is a type I transmembrane protein that was identified by mRNA analysis of activated versus resting mouse natural **regulatory T cells (Tregs)** [5] and also by homology to coinhibitory molecules such as **PD-1** [6]. VISTA bears features of both the B7 and CD28 families of immunoregulatory molecules and can act as both a ligand and a receptor [3,7,8]. The VISTA ECD is most homologous to the B7 family, which includes well-known immune checkpoint ligands such as **PD-L1** (Figure 1C). Whereas other B7 family members have an IgV-like and IgC-like domain, mouse and human VISTA contain a single unusually large IgV-like domain (Figure 1A) [2]. VISTA is also homologous to the T cell coinhibitory receptor PD-1, a member of the CD28 superfamily (Figure 1C). VISTA contains three C-terminal Src homology domain 3 (SH3) binding motifs (PxxP), whereas cytotoxic T lymphocyte-associated protein 4 (CTLA-4) and CD28 contain one and two SH3-binding motifs, respectively [9]. Human VISTA contains a Src homology domain 2 (SH2) binding motif (YxxQ), as well as multiple casein kinase 2 and phosphokinase C phosphorylation sites in the cytoplasmic domain (Figure 1A) [10]. These cytoplasmic motifs suggest that VISTA, as a receptor, can signal to VISTA-expressing cells in a manner akin to PD-1; however, the similarity between the VISTA and PD-L1 IgV domains, as well as the signaling potential of VISTA receptors, P-selectin glycoprotein ligand 1 (PSGL-1), and V-set and Ig domain-containing 3 (VSIG3) (Figure 1B), suggest that VISTA might also function as a ligand [9,11].

Binding Partners for VISTA

Human VISTA has two confirmed binding partners with immunosuppressive functions, PSGL-1 and VSIG3 [3,12], as well as a less well confirmed receptor, VSIG8 [12,13]. VISTA interacts with VSIG3 at physiological pH, but at acidic pH VISTA-expressing cells can bind to PSGL-1 on T cells. Both interactions result in inhibition of T cell function [3,12]. We focus here on the unique features of human VISTA and its immunologically relevant binding partners, VSIG3 and PSGL-1, because they suggest differential spatial expression patterns, and the pH of the TME might play an essential role in regulating VISTA functions *in vivo*.

VSIG3

VSIG3 is an Ig superfamily member that is expressed on a wide array of non-hematopoietic cells, but the immunosuppressive activity of VSIG3 has only recently been described [12]. Human and mouse VSIG3 contain an N-terminal IgV-like domain followed by an IgC-like domain, a transmembrane domain, and a cytoplasmic domain with a C-terminal PDZ-binding motif that might interact with cytoplasmic scaffolding proteins containing a PDZ domain (Figure 1B) [14]. VSIG3 has homology to adhesion receptors such as Coxsackie and adenovirus receptors and **endothelial cell-selective adhesion molecule (ESAM)**; an early study showed that human VSIG3 homophilic interactions appear to regulate cell aggregation, based on flow cytometry assays of conjugate formation [15]. In human total anti-CD3-activated T cells, the VSIG3–VISTA interaction *in vitro* led to reduced production of multiple cytokines including interleukin (IL)-2, IL-17, interferon γ (IFN-γ), chemokine (C-C motif) ligand 5 (CCL5), chemokine (C-C motif) ligand 3 (CCL3), and C-X-C motif chemokine 11 (CXCL11), supporting a role for VSIG3 as a possible negative immune checkpoint (Figure 2C) [12].

VSIG3 in Malignancy

The detailed mechanisms of how VSIG3 signaling can suppress **tumor-associated macrophage (TAM)-** and **tumor-infiltratinglymphocyte (TIL)**-mediated responses in tumors remain unknown. In normal tissue, human VSIG3 is most highly expressed in the testis and ovary, and at lower amounts in the brain, kidney, and skeletal muscle [14,16]. Human VSIG3 can be expressed by tumor cells, including gastric cancer cells and hepatoma cells [12,16]. Although knockdown of VSIG3 suppresses tumor growth *in vitro* in St-4 gastric cancer cells, the immunologic role of VSIG3 in tumors has not been established *in vivo* [16]. Whether the immunosuppressive signal from the VSIG3–VISTA interaction is delivered by tumor cells to myeloid cells and T cells is not clear [12]. In one study, the binding affinities of VISTA for VSIG3 and its other receptor, PSGL-1, were compared. At pH 7.4, the apparent binding affinity of VISTA for VSIG3 was 20 nM, whereas binding to PSGL-1 was undetectable [4]. By contrast, at pH 6.0, that is often seen in the TME, the apparent binding affinity for PSGL-1 was 4 nM, whereas the affinity for VSIG3 declined fourfold to 80 nM [4]. Although it is tempting to speculate that VSIG3 is the immunologically active partner for VISTA at neutral pH (Figure 2C) as opposed to PSGL1 at acidic pH, this remains hypothetical and needs to be shown experimentally. Of note, VSIG8 has also been reported to bind to VISTA, although binding to VSIG8 was not confirmed in one report [12,13].

PSGL-1

PSGL-1 is a well-established adhesion molecule that mediates human and mouse leukocyte trafficking by binding to P-selectin on activated endothelial cells through a rolling mechanism [17] (Figure 2A). Unlike VSIG3, PSGL-1 (encoded by the *SELPLG* gene) expression occurs primarily on hematopoietic cells [14,18]. Human PSGL-1 is highly expressed on almost all leukocytes, with lower expression on B cells [18]. Some non-hematopoietic cells, such as microvascular endothelial cells and epithelial cells of the fallopian tube, can also express human PSGL-1 [18]. The functional binding of human

PSGL-1 to selectins and VISTA is regulated by glycosylation and tyrosine sulfation, which are in turn regulated by lymphocyte activation [19,20]. It may be significant that human PSGL-1 has three tyrosines in the putative binding region whereas mouse has only two [3,21]. Of note, the unmodified PSGL-1 protein alone does not confer any functional activity to T cells [19,22].

PSGL-1 in Chronic Viral Infection

The role of PSGL-1 as an immune checkpoint receptor on 'exhausted' $CD4^+$ and $CD8^+$ T cells (**T cell exhaustion**) has been shown in mice chronically infected by lymphocytic choriomeningitis virus (LCMV) clone 13 (CL13) [23]. Following infection, there were more virus-specific $CD4^+$ T cells in the periphery in *Selplg*$^{-/-}$ mice relative to wild-type (WT) mice [23]. PSGL-1 engagement inhibited T cell receptor (TCR) activation, reduced IL-2 production, and upregulated other coinhibitory receptors such as PD-1. Even though *Selplg*$^{-/-}$ mice exhibited enhanced T cell responses to LCMV and resolved chronic LCMV infection sooner than WT infected animals, there was >50% mortality as a result of an overactive immune response [23]. This is similar to the mortality that has been observed in *Pdcd1*$^{-/-}$ mice in the LCMV infection model [24], providing the first evidence that PSGL-1 is an immune checkpoint [24]. When WT $CD8^+$ T cells were stimulated with the LCMV-specific GP33–41 peptide and IL-2, and PSGL-1 was ligated with anti-PSGL-1 mAb (clone 4RA10), the mice harbored fewer virus-specific $CD8^+$ T cells, and these had enhanced PD-1 expression relative to WT mice (Figure 2G) [23]. However, the ligand that engages PSGL-1 and inhibits anti-LCMV immune responses was not determined [23].

PSGL-1 in Malignancy

The role of PSGL-1 as an immune checkpoint has been clarified in conditions such as wound healing or in tumors, where the pH can be 5.85–6.5 [25–27]; it is reasonable to speculate that human PSGL-1 is a binding partner of human VISTA at the low pH that is commonly found in tumors (Figure 2D–F) [3]. An acidic pH-selective VISTA mAb that blocks the PSGL-1/VISTA interaction increases IFN-γ production, NF-κB phosphorylation, and cell proliferation of human $CD4^+$ T cells cocultured with VISTA-expressing cells *in vitro* [3]. At neutral pH there is little to no binding of PSGL-1 to VISTA; however, in acidic conditions one can speculate that the PSGL-1/VISTA pathway might be an important pathway inhibiting T cell activation (Figure 2D–F) [3]. However, few data directly address the role of PSGL-1 in tumor immunity, and much needs to be learned about this pathway *in vivo*. VISTA and PSGL-1 might function as both ligand and receptor, but we have yet to learn whether the VISTA/PSGL-1 interaction occurs only in *trans*, or whether it can also work in *cis* to inhibit activation [28]. Clearly, the immunologic activity of PSGL-1 is undergoing re-evaluation and PSGL-1 itself represents a potential therapeutic target.

Overlapping but Distinct Binding Sites for VISTA Receptors

Human VISTA is 279 amino acids in length, consisting of a 162-amino-acid ECD, a 21 amino acid transmembrane domain, and a 96 amino acid cytoplasmic domain with several notable features, namely (i) VISTA lacks any immunoreceptor tyrosine-based motif, unlike other CD28 family homologs such as PD-1 and CTLA-4 [10]. (ii) The ECD of VISTA

contains 10 β-strands, instead of the nine that typically make up an IgV domain (Figure 1D): the long length of the VISTA IgV domain, which is ~149 amino acids in length, is an outlier in the V-set (PF07686) Pfam database of 1873 V-set domains. The 3D structure of human VISTA has been published by three groups [2,3,29]. These structures show that the 10 β-strands adopt a β-sandwich conformation reminiscent of an IgV-like structure in which the H, A, G, F, C, and C′ strands comprise the front face, and the A′, B, E, and D strands form the back face in which the canonical Ig disulfide bond (Cys22–Cys114) (Figure 1D, inset 4) bridges the B and F strands. (iii) Between the C and C′ strands, VISTA contains a 21 residue protruding loop (C–C′ loop; yellow in Figure 1D), in sharp contrast to PD-L1 and other B7 family receptors that only contain a 4 residue loop connecting the C and C′ β-strands [2]. This ends with an extra helix composed of FQDL. (iv) VISTA contains an abundance of histidines that are concentrated in three clusters in the C–C′, D–E, and F–G loops [2,3], and these create a pH-sensitive charge switch that is part of the PSGL-1 binding site (Figure 1D, inset 1) [2,3]. VISTA contains two additional conserved disulfide bonds (C44/C178 and C83/C145) that are not present in other B7 family molecules [29]. (vi) The unusually long C–C′ loop has a uniquely oriented salt bridge (Arg90–Asp140) between the B and D strands that stabilizes the structure [29]. The H strand is secured by a disulfide bond to the A strand, resulting in a short stalk of ~9 amino acids. This likely orients VISTA such that the histidine-rich CDR-like region faces sideways on the cell surface instead of the usual outwards, and reduces the rotational freedom of the extracellular domain. The importance of the H strand has been further validated by deletion of the H strand or by mutation of the anchoring disulfide bond, which significantly reduced the inhibitory function of VISTA in T cell assays [29].

Structural and mutational analyses show that VSIG3 and PSGL-1 interact with overlapping but distinct regions of VISTA. Both interact with residues in the C strand (F68, K70), in the C–C′ loop and adjacent helix (R86, Q95), and in the F–G loop (H154), and PSGL-1 has additional interactions with histidines in the C–C′ and F–G loops (H100, H101, H153) (Figure 1D, inset 2) [2–4,29]. The protruding C–C′ loop, that is unique to VISTA, contains four residues (R86, R90, F94, Q95) which are essential for binding the VISTA antibody (VSTB). This mAb was used in a Phase I trial in patients with advanced cancers [2], but the trial was terminated and little is publicly known regarding the clinical outcomes or adverse effects of VSTB [8], or why the trial was terminated [8]. Of note, blocking VISTA with VSTB mAb, or mutating VISTA residues R86 and Q95 to alanine, reduced the binding of VISTA to VSIG3 relative to controls (Figure 1, inset 5) [2].

Two groups have highlighted the importance of an abundance of histidines in the ECD of VISTA, where histidine residues comprise 8.6% of its ECD, in striking contrast to the mean histidine content of 2.4% for type I transmembrane ECDs in UniProt [29]. The importance of this histidine rim is that, under acidic conditions, the amino group on these histidines is protonated, creating a positively charged region that allows interaction with negatively charged PSGL-1 (Figure 3) [3]. Three histidine residues H153, H154, and H155, that are located on the nonprotruding F-G loop, are pivotal for binding to PSGL-1. Replacement of this triple-histidine cluster with positively charged arginines enables VISTA to bind to PSGL-1 at pH 7.4, while not affecting its binding at pH 6.0 [3]. Moreover, substitution of this triple-histidine cluster with negatively charged aspartic acid eliminates VISTA binding

[3]. These three histidines are also essential for binding VISTA.18, an acidic pH-selective anti-VISTA mAb that blocks binding to PSGL-1. This pH selectivity allows the VISTA.18 mAb to preferentially bind in the acidic TME [3] (Figure 1E). Replacing this triple-histidine cluster with alanines also reduced the inhibitory function of VISTA in antigen-specific T cell assays [29].

VISTA Expression and Function as a Receptor or a Ligand

The role of VISTA as an immune checkpoint is illustrated by *Vsir*$^{-/-}$ mice that develop spontaneous autoimmunity resembling **systemic lupus erythematosus (SLE)** [30], and by exacerbated T cell-mediated immune pathology in multiple mouse disease models such as **graft-versus-host disease (GVHD), experimental allergic encephalomyelitis (EAE),** and **rheumatoid arthritis (RA)** [11]. In nonmalignant conditions, VISTA is primarily expressed in hematopoietic tissues (i.e., spleen, thymus, and bone marrow) or in tissues with abundant leukocyte infiltration (i.e., lung) in mice [5,6]. Like PD-L1, both mouse and human VISTA are expressed on both lymphoid and myeloid cells [31]. There is weak expression in non-hematopoietic tissues (i.e., heart, kidney, brain, muscle, testis, embryo, and ovary) [5,6]. Much like PD-L1 and some other B7 family members, VISTA is highly expressed on trophoblast cells in human placenta [31]. Of note, VISTA expression can vary across anatomical location and cancer types, and is increased by anti-PD-1 or anti-CTLA-4 immune checkpoint treatments in some cancer types such as melanoma and prostate cancer [1,32].

VISTA in Normal Physiology

In the hematopoietic compartment, there are varying amounts of VISTA expression, depending on the cell type, maturation, location, and species. VISTA expression in humans appears to be similar to that of mice on **myeloid-derived suppressor cells (MDSCs)**, TAMs, and TILs in different cancer types such as kidney cancer and melanoma [1,7,33–37]. VISTA is most highly expressed in the myeloid compartment, and the pattern of expression in humans shows that activated or ‘inflammatory’ myeloid cells express more VISTA than resting monocytes, and that immunosuppressive myeloid cells express the highest amount of VISTA (MDSCs compared with TAMs) [31,34,35]. VISTA is expressed by mouse and human microglia, the major myeloid cell in the central nervous system (CNS) [38]. Thus, in developing therapeutics to target VISTA for autoimmune or oncological indications, it will be crucial to monitor potential adverse events in the CNS owing to activation or depletion of microglia [38]. The expression of mouse and human VISTA on lymphocytes is lower than on myeloid cells, and follows an interesting pattern that might suggest clinical relevance [5]. Specifically, its expression in the murine thymus is negative on $CD4^+CD8^+$ double-positive thymocytes, low on $CD4^+$ single positive cells, and higher on $CD8^+$ single-positive cells [5]. In peripheral lymphoid organs such as the spleen and lymph nodes, VISTA expression is found on naïve $CD4^+$ ($CD44^{lo}CD62L^{hi}$) T cells and Tregs, but less on $CD4^+$ ($CD44^{hi}CD62L^{lo}$) memory-like T cells [11]. Conditional deletion of *Vsir* in mouse $CD4^+$ T cells showed that VISTA can enforce T cell quiescence in naïve T cells. *CD4–Cre Vsir*$^{-/-}$ mice exhibited decreased naïve T cells and more memory-like T cells compared with WT mice, as demonstrated by gene enrichment analysis of single-cell RNA-seq of lymphocytes

in peripheral immune tissues [11]. VISTA expression on $CD4^+$ naïve mouse T cells is consistent with VISTA being a regulator of peripheral tolerance given that VISTA expression diminishes following the activation of $CD4^+$ T cells [11]. By contrast, both mouse and human VISTA expression on other lymphocyte subsets such as B lymphocytes and natural killer (NK) cells is almost negligible [5].

VISTA in Malignancy

Immune checkpoint proteins are often overexpressed in cancer. Among the tumor types in The Cancer Genome Atlas (TCGA), human VISTA is most highly expressed in epithelioid mesotheliomas including tumor cells and inflammatory cells [39,40]. Higher VISTA expression has been associated with better clinical outcomes, whereas PD-L1 has been associated with worse outcomes in epithelioid mesothelioma cancer patients [40]. In most human cancers and murine models, VISTA is predominantly expressed on immune cells in the TME, although VISTA has also been described on tumor cells in human lung, kidney, colorectal, endometrial, and ovarian cancers [33,34,36,41]. However, VISTA expression on murine cancer cell lines is rare. In murine melanoma *in vivo*, when VISTA is overexpressed in D4M UV2 tumors, VISTA expression has been associated with both PD-L1 expression on tumor cells and with other immunosuppressive pathways such as recruitment of $Foxp3^+$ Tregs, downregulation of MHC class I and MHC class II, and activation of β-catenin [32,42]. This association has also been seen in human melanoma by immunohistochemistry [32,42]. In the TME, VISTA expression has been reported to be particularly high in murine $CD11b^+$ myeloid cells in RENCA kidney cancer [34], CT26 colon cancer [35], B16 melanoma [35], and MB49 bladder cancer [35]; in human $CD11b^+$ myeloid cells in kidney cancer [34], colorectal cancer [36], pancreatic ductal adenocarcinomas (PDACs) [37]; and in the human $CD68^+$ myeloid compartment in colorectal cancer [1]. In human acute myeloid leukemia (AML), VISTA has been reported to be expressed on AML blasts and MDSCs, but it is uncertain whether VISTA is functioning as an immunosuppressor or is merely a marker of the myeloid origin of the cancer [7].

TILs have higher VISTA expression than T cells in normal lymphoid structures [35]. In addition, VISTA is most strongly expressed in the most hypoxic region of mouse colon CT26 tumors [43]. Indeed, hypoxia-inducible factor 1α (HIF-1α) can upregulate VISTA expression through hypoxia response elements in the *Vsir* promoter [43]. This has suggested that the hypoxic TME might create a specialized niche where the acidity could potentially maximize VISTA immunosuppressive activity; however, this is a hypothesis that remains to be rigorously tested [10].

Of note, the pattern of VISTA expression on immune cells differs across cancers. For example, in human non-small cell lung cancer (NSCLC), VISTA expression appears to be different from most other human cancers reported [1,33,34,36,37]. On immune cells in human NSCLC, VISTA expression is significantly higher in $CD3^+$ T cells than in $CD68^+$ macrophages, which is different from most other cancers [33]. This distinction might potentially be attributed to different antibody clones and quantitation methods, or might be due to the lymphocyte-enriched nature of the human NSCLC TME [44], compared with the highly myeloid cell infiltrates in other human cancers such as PDAC, clear-cell renal cell

carcinoma (ccRCC), and colorectal carcinoma (CRC) [45–47]. Although VISTA can be expressed on tumor cells, the majority of its expression is on immune cells; furthermore, TME factors such as hypoxia can increase the expression of VISTA, potentially promoting immune suppression through VISTA-dependent pathways.

VISTA on Immune Cells

Given the range of VISTA expression across cancers, and the development of therapeutics targeting VISTA and its binding partners, it is timely to review the data on which cells are affected by VISTA deficiency or blockade.

T Lymphocytes

VISTA is essential for the maintenance of T cell quiescence [11]. VISTA and PD-1 mediate nonredundant pathways that modulate T cell responses, given that the magnitude of T cell responses to foreign antigens has been shown to be synergistically higher in *Vsir*$^{-/-}$*Pdcd1*$^{-/-}$ mice relative to WT mice [48]. VISTA expression on naïve CD4^{+} T cells and **γδ T cells** inhibits their autoreactivity, thereby preventing T cell activation in the absence of foreign antigenic stimulation [11,49]. Moreover, mouse VISTA expression on CD4^{+} T cells declines as naïve CD4^{+} T cells engage foreign antigens and differentiate into memory CD4^{+} T cells [11]. In addition, relative to WT mice, *Vsir*$^{-/-}$ mice exhibit impaired **activation-induced cell death (AICD)**, leading to less peripheral T cell deletion and development of autoimmune phenotypes [11,30]. Furthermore, *Vsir*$^{-/-}$ skews CD4^{+} T cells from a quiescent phenotype – manifested by a quiescence gene regulator module (such as Krüppel-like factor 2, *Klf2*) – to a more **stem cell memory-like gene module** (such as Krüppel-like factor 3, *Klf3*) [11]. *Ex vivo* analysis of immune cells in a mouse model of psoriasis showed that *Vsir*$^{-/-}$ mice had increased peripheral expansion relative to WT mice of CD27^{-} γδ T cells as a result of unrestricted STAT5 (signal transducer and activator of transcription 5) activation downstream of IL-7R signaling [49]. Although VISTA expression regulates peripheral homeostasis of T cells, VISTA expression in the myeloid compartment can also contribute to the regulation of T cell activation.

Myeloid-Derived Cells and Dendritic Cells

In both human and mouse, VISTA expression is higher in myeloid cells than in lymphocytes [9]. Based on an analysis of peritoneal macrophages from *Vsir*$^{-/-}$ mice – showing augmented **Toll-like receptor (TLR)**-mediated proinflammatory cytokine production relative to WT mice – VISTA deficiency has been deemed to result in increased steady-state myeloid activation and production of inflammatory cytokines, suggesting that VISTA might function to maintain quiescence in myeloid cells [50]. In lipopolysaccharide (LPS)-induced septic shock mouse models, VISTA agonist activity can epigenetically reprogram macrophages towards a reduction in proinflammatory cytokines IL-6, tumor necrosis factor α (TNF-α), and IL-12, and an increase in anti-inflammatory mediators including IL-10, interleukin-1 receptor antagonist (IL-1RA), miR-221, merTK, immune-responsive gene 1 (IRG1), and the A20 deubiquitinase that negatively regulates NF-κB relative to an isotype control [51]. Moreover, anti-VISTA agonistic antibodies may represent therapeutic candidates for treating autoimmune diseases such as cutaneous lupus erythematosus and

SLE because they can induce a tolerogenic and anti-inflammatory profile in both mouse and human macrophages [30,51].

In addition, VISTA can inhibit myeloid differentiation primary response 88 (MyD88)-dependent TLR signaling and the production of proinflammatory cytokines by myeloid cells because the therapeutic benefit conferred by anti-VISTA blockade is diminished in *Myd88*$^{-/-}$ EG7 thymoma tumor-bearing mice compared with WT (Figure 2B) [50]. Moreover, in imiquimod (IMQ)-induced psoriasis in *Vsir*$^{-/-}$ mice, there is enhanced TLR signaling that can induce dendritic cells (DCs) to produce higher quantities of IL-23 relative to WT mice, in turn contributing to IL-17A production by priming γδ T cells and T helper 17 (Th17) cells [49]. Similarly, *Vsir*$^{-/-}$ mouse splenic DCs and peritoneal macrophages stimulated with the TLR-7 agonist R848 have exhibited enhanced TLR signaling relative to WT mice, as evidenced by increased phosphorylation of both extracellular signal-regulated kinases (Erk1/2) and c-Jun N-terminal kinase (Jnk1/2) [49,50]. In this study, relative to controls, VISTA antibody blockade led to a higher number of inflammatory DCs, higher expression of IL12p40, and inhibition of **monocytic MDSCs (mMDSCs)** and **granulocytic MDSCs (gMDSCs)** in B16 melanoma tumors in mice, resulting in an increase in IFN-γexpressing TILs [50]. VISTA is upregulated particularly on MDSCs in mouse and human tumors, and can contribute to their immunoinhibitory function, for example, in kidney cancer, CT26 colon carcinoma, B16 melanoma, and MB49 bladder cancer [34,35,43]. A high frequency of VISTA^{+} cells among intratumoral myeloid cells was positively associated with MDSC infiltration – which carries a negative prognosis and is negatively associated with CD8^{+}/CD4^{+} T cell infiltration and cytolytic activity of CD8^{+} TILs – in human kidney cancer [34]. Moreover, *Vsir*$^{-/-}$ or blockade with VISTA mAb in peritoneal macrophages isolated from B16 melanoma murine tumors was reported to modulate TLR signaling via changes in polyubiquitination, including lowered K48 (proteasome degradation) and enhanced K63-linked polyubiquitination, which activated **tumor necrosis factor receptor (TNFR)-associated factor 6 (TRAF6)** relative to controls [50]. VISTA activity also reduced transforming growth factor-β activated kinase I (TAK1) phosphorylation that modulated TRAF6 signaling [50]. Thus, a combination of VISTA-blocking antibody with an immunostimulatory strategy might help to improve the therapeutic efficacy of cancer immunotherapy, although this needs to be tested further.

VISTA in the Context of Immunotherapy

High VISTA expression has been associated with poor survival in colon cancer patients [43]. The immunosuppressive function of VISTA on both lymphocytes and myeloid cells, and the abundant expression of VISTA on TILs, suggest that VISTA-blockade therapy may have potential broad clinical applicability. The majority of models describing effective VISTA therapy rely on a combination approach. VISTA and PD-L1 combination therapy in a CT26 colon cancer mouse model led to tumor regression and long-term survival in all recipient mice, which was in sharp contrast to either monotherapy (12.5% for VISTA mAb monotherapy and 37.5% for PD-L1 mAb monotherapy) [48]. Combination treatment with VISTA and PD-L1 mAbs also showed a significant survival advantage and tumor eradication in B16 tumor-bearing mice conditioned with low-dose irradiation (250 rads) and treated with four doses of granulocyte-macrophage colony-stimulating factor (GM-CSF)-secreting

cellular vaccine (GVAX) before mAb treatment [48]. In another study, combining VISTA mAb 13F3 with a TLR vaccine or TLR agonists (CpG and R848) resulted in long-term tumor-free survival in 50% of B16 tumor-bearing mice. By contrast, monotherapy with the TLR vaccines or VISTA mAb blockade only transiently delayed tumor growth in B16 melanoma tumor-bearing mice, without long-lasting effects [50]. VISTA blockade using the 13F3 blocking mAb combined with a peptide vaccine containing agonistic CD40 antibody, TLR agonists, and tumor antigen peptides has shown promising synergistic effects for treating both early (2 day) and established (7 day) B16 melanoma tumors [35]. An orally administered small-molecule inhibitor, CA-170, was reported to bind to the H-strand of VISTA, and also to block PD-L1 and PD-L2 [52]. In this study, CA-170 enhanced T cell immune responses and the production of IFN-γ [52]. CA-170 is in clinical development; however, a recent study showed minimal to no binding of CA-170 to human VISTA by time-resolved fluorescence energy-transfer assay [53]. In this study, another small-molecule inhibitor, compound III, inhibited VISTA immunosuppressive function, as measured by increased IFN-γ and TNF-α secretion by Jurkat T cells cocultured with VISTA-positive ovarian cancer cell lines. Docking and mutational analysis showed that compound III interacted with VISTA residues F94, R159, and E157, with a strong hydrophobic interaction with Y69 and H153 [53]. Thus, small-molecule inhibitors are under development as putative VISTA therapeutics in addition to antagonist and agonist antibodies.

Understanding VISTA Therapeutic mAbs

VISTA Antagonists

Given the significance of VISTA in disease, it is important to understand the functional mechanisms of VISTA mAbs. There are three VISTA antagonist mAbs in development: (i) VSTB112, (ii) P1–068767 (BMS-767), and (iii) SG7. Each of the three mAbs has been reported to enhance T cell activation in functional assays [4,54,55]. VSTB112 was used in a Phase I trial in patients with advanced cancer (NCT02671955[i]) (Figure 1D, inset 2) [2], but the trial was terminated and little is publicly known regarding the clinical outcomes, adverse effects of VSTB, or why the trial was terminated [7]. VSTB112 binds to an epitope containing the C–C′ loop and the adjacent helix that are also important for the interaction of VISTA with VSIG3 and PSGL-1 [4,54]. All three antagonistic mAbs block VISTA interaction with human PSGL-1 and VSIG3 with similar effectiveness [4]. VSTB112, BMS-767, and SG7 cross-block each other, but the crucial amino acids on VISTA that are responsible for antibody binding differ [4]. Comparing antibody characteristics and epitope overlap across SG7, BMS-767, and VSTB-112 mAbs raises interesting questions for the clinical development of therapeutic VISTA antibodies. First, the SG7 mAb has a 25–50-fold stronger affinity for human VISTA than either BMS-767 or VSTB-112 [4]. The SG7 mAb was selected by multiple rounds of yeast display and is unique in its cross-species reactivity for human, cynomolgus monkey, and mouse VISTA, allowing *in vivo* testing of the clinical candidate in mice [4]. The other two antagonistic VISTA mAbs only bind to human VISTA and will need to be modeled in human VISTA knock-in mice [3,54,55]. Second, the BMS-767 mAb is the only pH-selective blocking antibody, and blocks PSGL-1 and VSIG3

[i] https://clinicaltrials.gov/ct2/show/NCT02671955

only at pH 6.0 [4]. BMS-767 has been shown to home to tumor sites with low pH, thereby potentially reducing any non-tumor reactivity and adverse effects [55]. H100 and H155 are important for BMS-767 binding and mediate the acidic pH-selective binding of BMS-767 because most of the contact residues in the C–C′ loop and adjacent helix are identical for VSTB-112 and SG7 mAbs. Third, despite overlapping binding epitopes of SG7, BMS-767, and VSTB-112, H154 in the F–G loop is the only common contact residue among these mAbs. Fourth, the mAbs differ in their engagement of the Fc receptor (FcR), and BMS-767 and VSTB-112 have an active Fc region whereas SG7 bears a 'dead' Fc [4,54,55]. A form of SG7 with an active Fc showed more depletion of myeloid cells in B16F10, MC38, and 4T1 tumor models, but was no more effective at slowing tumor growth than the form with 'dead' Fc. Thus, SG7 may have less toxicity than the other mAbs; however, this remains to be tested further [4]. Given the high expression of VISTA on many myeloid cells, part of the *in vivo* effects of VISTA blockade might be myeloid dependent, and rigorously testing the effects of these mAbs in myeloid functional assays is therefore warranted.

VISTA Agonists

Agonistic anti-VISTA mAbs enhance VISTA activity, thereby downregulating immune responses, and thus might be considered as candidates for the treatment of autoimmune diseases such as SLE and GVHD [11]. Indeed, VISTA agonist mAbs can enhance peripheral T cell tolerance through increased AICD [56]. Agonist mAbs have been shown to inhibit proinflammatory cytokine production in mouse models of autoimmune disease including NZB/W F1 lupus, K/BxN arthritis, IMQ-induced psoriasis, GVHD, and concanavalin-induced autoimmune hepatitis (AIH) [11]. 8G8 and INX803 were the most promising mouse and human VISTA agonist mAbs, respectively [56]. Epitope-binding assays suggested that VISTA agonist mAbs bind to an epitope containing the α3 helix, F strand, F–G loop, and G strand [56]. Moreover, VISTA agonist mAbs have been presumed to transduce VISTA signals to inhibit immune responses, but this remains to be assessed, and it will be interesting to test whether these agonists can strengthen the ligand interaction as a mechanism to enhance the immunosuppressive functions of VISTA.

A Strategy To Reduce VISTA Immunoinhibitory Activity: pH Regulation in the TME

Decreased extracellular pH (pHe) is a hallmark of solid tumors and is associated with tumor progression, metastasis, and immunosuppression [57]. Given that VISTA binding to PSGL-1 and its immunoinhibitory activity are enhanced at the acidic pH of the TME, increasing the pH of the TME might represent a strategy to reduce the immunoinhibitory activity of VISTA. An acidic microenvironment created by lactic acid secretion can result in dysfunctional T cells by reduced expression of nuclear factor of activated T cells (NFAT) which results in less IFN-γ production [58,59]. The combination of low pHe and high intracellular pH (pHi) in tumors is achieved by elevated transmembrane acid extrusion [60]. The direct regulators of pH in the TME can be divided into regulators of cellular metabolism, that generate intracellular acidic products such as lactate and H^+, and the transporters that move lactate and H^+ into the extracellular space (Figure 4) [26]. The H^+/ $HCO3^-$ transporters that regulate intracellular and extracellular acidity include Na^+/ H^+

exchanger 1 (NHE1), $H^+/HCO3^-$ transport channel (NBC), vacuolar-H^+-ATPase (V-ATPase), and monocarboxylate transporters (MCTs) [26]. Inhibitors of $H^+/HCO3^-$ transporters might be a particularly promising means to reinvigorate antitumor lymphocytes that are inhibited by the low pH in the TME, when combined with VISTA or other checkpoint mAbs in the optimal sequence. Some of these transporters are in clinical development in oncology (Table 1 and Box 1).

Indirect Metabolic Mechanisms That Increase Extracellular Acidity

Indirect metabolic mechanisms that decrease pHe include hypoxia, oncogene activity, and the **Warburg effect** (Figure 4 and Box 2) [10]. Hypoxia is a major driving force within the tumor through both HIF-dependent and -independent mechanisms. In addition to the TME, lymph nodes (LNs), wound-healing sites, and bone fractures also have an acidic pH, making them immunosuppressive niches and likely sites of VISTA activity [3,61–63]. The paracortical region of the LN is acidic, a possible result of T cell glycolytic activity [61]. This acidic microenvironment has been shown to inhibit murine $CD8^+$ T cell effector functions and prevent cytokine production at a post-translational step. Once at physiologic pH outside the LN, T cells can regain their functionality [61]. The acidic pHe in bone fractures is associated with enhanced proinflammatory cytokine and cathepsin B production, leading to acidic pH-dependent osteoblast death [63]. Human cutaneous wound healing is characterized by a pH decline from an initial 8–8.8 at time of injury to 6.0 after the beginning of epidermal barrier re-establishment [64]. Infiltrating neutrophils can lower the pH in wounds by upregulating NHE1 and CA IV/IX expression [62]. Indeed, tumors have been described as ‘a wound that does not heal’ [65]. These are examples where acidic pH appears to downregulate lymphocyte activity to allow normal function and repair of tissue. We hypothesize that selectively manipulating the pH of the TME might be an alternative way to modulate VISTA activity [61,66].

Concluding Remarks

VISTA immunoinhibitory activity enforces quiescence on naïve T and myeloid cells. Both mouse and human VISTA are predominantly expressed on hematopoietic cells, where the highest expression levels are seen in the myeloid compartment, including monocytic and granulocytic cells, and weaker expression on T cells [9]. In addition, VISTA can be expressed on a variety of tumors. VISTA mAbs with different immune functionalities (i.e., antagonists and agonists) have opened up future directions for potentially treating particular cancers and autoimmune diseases. The FcR-binding activity of the VISTA mAb or lack thereof may be a key factor in achieving optimal efficacy in specific therapeutic modalities; therefore, rigorous safety and efficacy testing are still required. The complexity of VISTA, that acts as both a ligand and a receptor, and of VISTA signaling in myeloid cells, might reveal new insights into its potential role as a major immunosuppressive pathway in the TME (see Outstanding Questions). This might need to be examined by approaches that include a thorough analysis of the spatial localization of VISTA/PSGL-1/ VSIG3-expressing cells in the TME, and a more complete understanding of the downstream signaling pathways of these three checkpoints. Moreover, the pH dependence of VISTA/PSGL-1 binding and acidity-induced immunosuppression shifts the focus to targeting the biochemical processes

that can alter pH. The low pH of tumors might be leveraged to target pH-selective antibodies that are more active in the acidic TME. In addition, future studies should aim to investigate whether druggable pH regulators that increase the pHe of the TME might alleviate VISTA-mediated immunosuppression and enhance the activity of combination cancer therapies with other immune checkpoint blockers such as PD-1 mAbs, or potentially cancer vaccines.

Acknowledgments

This work was supported by the National Cancer Institute (P50CA101942 to K.M.M. and G.J.F.), P50CA206963 (G.J.F.), R01CA234018 (G.J.F.), and an Advanced Discovery Award (2019–1517) from the Kidney Cancer Association (K.M.M. and G.J.F.).

Glossary

Activation-induced cell death (AICD)
programmed cell death where activation of the T cell receptor results in apoptosis

Experimental autoimmune encephalomyelitis (EAE)
a disease in an animal model (e.g., rodents) that is commonly employed as a model for multiple sclerosis (MS), an inflammatory demyelinating disease of the central nervous system (CNS)

Endothelial-cell selective adhesion molecule (ESAM)
a member of the immunoglobulin superfamily that mediates homophilic interactions between endothelial cells

Granulocytic MDSCs (gMDSCs)
a subset of MDSCs that have a morphology similar to granulocytes.

Graft-versus-host disease (GVHD)
a condition that develops when a donor transplant immune cells attack the tissues of the recipient

Myeloid-derived suppressor cells (MDSCs)
a heterogeneous group of immune cells from the myeloid lineage that expand under conditions such as chronic infection, autoimmunity, and cancer. Unlike TAMs, they lack MHC-II expression and have significant immunosuppressive properties in an antigen-nonspecific manner

Monocytic MDSCs (mMDSCs)
a subset of MDSCs that have a morphology similar to monocytes

PD-1/PD-L1 immune checkpoint
an immunoinhibitory pathway that is important for peripheral tolerance and attenuation of immune responses; the pathway is frequently used by tumors to evade immune attack

Programmed death ligand1 (PD-L1)
one of the ligands for PD-1 that inhibits immune responses

Programmed cell death protein (PD-1) (CD279)
a cell-surface receptor for immunoinhibitory signaling by PD-L1 and PD-L2; PD-1 is frequently targeted in cancer immunotherapy

Regulatory T cells (Tregs)
a subset of $CD4^+$ T cells characterized by Foxp3 expression; Tregs mediate T cell peripheral tolerance

Rheumatoid arthritis (RA)
a condition characterized by synovial fluid inflammation and autoantibody production

Stem cell memory-like gene module
a set of expressed genes that enforce a memory-like phenotype in stem cells

Systemic lupus erythematosus (SLE)
a complex multisystem autoimmune disorder that results from widespread immune complex deposition and secondary tissue injury. SLE is characterized by the presence of antinuclear antibodies

γδ T cells
a subset of T cells whose TCR is composed of a γ and a δ chain.

Tumor-associated macrophages (TAMs)
a class of myeloid immune cells that can polarize in different milieus in the tumor, and that can both suppress antitumor immunity and promote tumor progression

Tumor-infiltrating lymphocytes (TILs)
lymphocytes that are found within the tumor tissue

Tumor necrosis factor receptor (TNFR)-associated factor 6 (TRAF6)
intracellular protein that mediates signaling through the TNFR and TLR superfamilies; for example, TRAF6 can regulate the activation of both MAPKs/AP-1 and NF-κB through MyD88-dependent TLR signaling

Toll-like receptor (TLR)
a family of receptors that recognize structural patterns in pathogens and damaged tissues and activate the innate immune response

T cell exhaustion
a T cell differentiation state produced by prolonged antigen stimulation; exhaustion is characteristic of chronic infections and cancer. Exhaustion is mediated by epigenetic changes and is characterized by progressive loss of T cell effector functions

Warburg effect
a modified cellular metabolism that is frequently used by cancer cells and that involves preferential glycolysis and biomass synthesis instead of oxidative phosphorylation

References

1. Gao J. et al. (2017) VISTA is an inhibitory immune checkpoint that is increased after ipilimumab therapy in patients with prostate cancer. Nat. Med. 23, 551–555 [PubMed: 28346412]
2. Mehta N. et al. (2019) Structure and junctional binding epitope of V-domain Ig suppressor of T cell activation. Cell Rep. 28, 2509–2516 [PubMed: 31484064]
3. Johnston RJ et al. (2019) VISTA is an acidic pH-selective ligand for PSGL-1. Nature 574, 565–570 [PubMed: 31645726]
4. Mehta N. et al. (2020) An engineered antibody binds a distinct epitope and is a potent inhibitor of murine and human VISTA. Sci. Rep. 10, 15171
5. Wang L. et al. (2011) VISTA, a novel mouse Ig superfamily ligand that negatively regulates T cell responses. J. Exp. Med. 208, 577–592 [PubMed: 21383057]
6. Flies DB et al. (2011) A monoclonal antibody specific for the programmed death-1 homolog prevents graft-versus-host disease in mouse models. J. Immunol. 187, 1537–1541 [PubMed: 21768399]
7. Wang L. et al. (2018) VISTA is highly expressed on MDSCs and mediates an inhibition of T cell response in patients with AML. Oncoimmunology 7, e1469594
8. ElTanbouly MA et al. (2020) VISTA: coming of age as a multilineage immune checkpoint. Clin. Exp. Immunol. 200, 120–130 [PubMed: 31930484]
9. Nowak EC et al. (2017) Immunoregulatory functions of VISTA. Immunol. Rev. 276, 66–79 [PubMed: 28258694]
10. Mahoney KM and Freeman GJ (2020) Acidity changes immunology: a new VISTA pathway. Nat. Immunol. 21, 13–16 [PubMed: 31822869]
11. ElTanbouly MA et al. (2020) VISTA is a checkpoint regulator for naïve T cell quiescence and peripheral tolerance. Science 367, eaay0524
12. Wang J. et al. (2019) VSIG-3 as a ligand of VISTA inhibits human T-cell function. Immunology 156, 74–85 [PubMed: 30220083]
13. Molloy M. et al. Immunext Inc. Identification of VSIG-8 as the putative VISTA receptor and its use thereof to produce VISTA/ VSIG-8 modulators, WO 2016/090347 A1
14. Suzu S. et al. (2002) Molecular cloning of a novel immunoglobulin superfamily gene preferentially expressed by brain and testis. Biochem. Biophys. Res. Commun. 296, 1215–1221 [PubMed: 12207903]
15. Harada H. et al. (2005) BT-IgSF, a novel immunoglobulin superfamily protein, functions as a cell adhesion molecule. J. Cell. Physiol. 204, 919–926 [PubMed: 15795899]
16. Watanabe T. et al. (2005) Identification of immunoglobulin superfamily 11 (IGSF11) as a novel target for cancer immunotherapy of gastrointestinal and hepatocellular carcinomas. Cancer Sci. 96, 498–506 [PubMed: 16108831]
17. Ley K. et al. (2007) Getting to the site of inflammation: the leukocyte adhesion cascade updated. Nat. Rev. Immunol. 7, 678–689 [PubMed: 17717539]
18. Laszik Z. et al. (1996) P-selectin glycoprotein ligand-1 is broadly expressed in cells of myeloid, lymphoid, and dendritic lineage and in some nonhematopoietic cells. J. Investig. Med. 44, 3010–3021
19. Vachino G. et al. (1995) P-selectin glycoprotein ligand-1 is the major counter-receptor for P-selectin on stimulated T cells and is widely distributed in non-functional form on many lymphocytic cells. J. Biol. Chem. 270, 21966–21974
20. Pouyani T. and Seed B. (1995) PSGL-1 recognition of P-selectin is controlled by a tyrosine sulfation consensus at the PSGL-1 amino terminus. Cell 83, 333–343 [PubMed: 7585950]
21. Thatte A. et al. (2002) Binding of function-blocking mAbs to mouse and human P-selectin glycoprotein ligand-1 peptides with and without tyrosine sulfation. J. Leukoc. Biol. 72, 470–477 [PubMed: 12223514]
22. Snapp KR et al. (1997) P-selectin glycoprotein ligand-1 is essential for adhesion to P-selectin but not E-selectin in stably transfected hematopoietic cell lines. Blood 89, 896–901 [PubMed: 9028320]

23. Tinoco R. et al. (2016) PSGL-1 is an immune checkpoint regulator that promotes T cell exhaustion. Immunity 44, 1190–1203 [PubMed: 27192578]
24. Barber DL et al. (2006) Restoring function in exhausted CD8 T cells during chronic viral infection. Nature 439, 682–687 [PubMed: 16382236]
25. Gethin G. (2007) The significance of surface pH in chronic wounds. Wounds UK 3, 52–56
26. Corbet C. and Feron O. (2017) Tumour acidosis: from the passenger to the driver's seat. Nat. Rev. Cancer 17, 577–593 [PubMed: 28912578]
27. Park JG et al. (2020) Kidney residency of VISTA-positive macrophages accelerates repair from ischemic injury. Kidney Int. 97, 980–994 [PubMed: 32143848]
28. Chaudhri A. et al. (2018) PD-L1 Binds to B7–1 only in cis on the same cell surface. Cancer Immunol. Res. 6, 921–929 [PubMed: 29871885]
29. Slater BT et al. (2020) Structural insight into T cell coinhibition by PD-1H (VISTA). Proc. Natl. Acad. Sci. U. S. A. 117, 1648–1657 [PubMed: 31919279]
30. Han X. et al. (2019) PD-1H (VISTA)-mediated suppression of autoimmunity in systemic and cutaneous lupus erythematosus. Sci. Transl. Med. 11, eaax1159
31. Lines JL et al. (2014) VISTA is an immune checkpoint molecule for human T cells. Cancer Res. 74, 1924–1932 [PubMed: 24691993]
32. Kakavand H. et al. (2017) Negative immune checkpoint regulation by VISTA: a mechanism of acquired resistance to anti-PD-1 therapy in metastatic melanoma patients. Mod. Pathol. 30, 1666–1676 [PubMed: 28776578]
33. Villarroel-Espindola F. et al. (2018) Spatially resolved and quantitative analysis of vista/pd-1h as a novel immunotherapy target in human non-small cell lung cancer. Clin. Cancer Res. 24, 1562–1573 [PubMed: 29203588]
34. Hong S. et al. (2019) Analysis of VISTA expression and function in renal cell carcinoma highlights VISTA as a potential target for immunotherapy. Protein Cell 10, 840–845 [PubMed: 31236852]
35. Le Mercier I. et al. (2014) VISTA regulates the development of protective antitumor immunity. Cancer Res. 74, 1933–1944 [PubMed: 24691994]
36. Xie S. et al. (2018) Expression of the inhibitory B7 family molecule VISTA in human colorectal carcinoma tumors. Cancer Immunol. Immunother. 67, 1685–1694 [PubMed: 30128738]
37. Blando J. et al. (2019) Comparison of immune infiltrates in melanoma and pancreatic cancer highlights VISTA as a potential target in pancreatic cancer. Proc. Natl. Acad. Sci. U. S. A. 116, 1692–1697 [PubMed: 30635425]
38. Borggrewe M. et al. (2018) VISTA expression by microglia decreases during inflammation and is differentially regulated in CNS diseases. Glia 66, 2645–2658 [PubMed: 30306644]
39. Hmeljak J. et al. (2018) Integrative molecular characterization of malignant pleural mesothelioma. Cancer Discov. 8, 1549–1565
40. Muller S. et al. (2020) V-domain Ig-containing suppressor of T-cell activation (VISTA), a potentially targetable immune checkpoint molecule, is highly expressed in epithelioid malignant pleural mesothelioma. Mod. Pathol. 33, 303–311 [PubMed: 31537897]
41. Mulati K. et al. (2019) VISTA expressed in tumour cells regulates T cell function. Br. J. Cancer 120, 115–127 [PubMed: 30382166]
42. Rosenbaum SR et al. (2020) FOXD3 regulates VISTA expression in melanoma. Cell Rep. 30, 510–524 [PubMed: 31940493]
43. Deng J. et al. (2019) Hypoxia-induced VISTA promotes the suppressive function of myeloid-derived suppressor cells in the tumor microenvironment. Cancer Immunol. Res. 7, 1079–1090 [PubMed: 31088847]
44. Stankovic B. et al. (2018) Immune cell composition in human non-small cell lung cancer. Front. Immunol. 9, 3101 [PubMed: 30774636]
45. Candido JB et al. (2018) CSF1R^{+} macrophages sustain pancreatic tumor growth through T cell suppression and maintenance of key gene programs that define the squamous subtype. Cell Rep. 23, 1448–1460 [PubMed: 29719257]
46. Mier JW (2019) The tumor microenvironment in renal cell cancer. Curr. Opin. Oncol. 31, 194–199 [PubMed: 30985497]

47. Toor SM et al. (2016) Increased levels of circulating and tumorinfiltrating granulocytic myeloid cells in colorectal cancer patients. Front. Immunol. 7, 560 [PubMed: 28008330]
48. Liu J. et al. (2015) Immune-checkpoint proteins VISTA and PD-1 nonredundantly regulate murine T-cell responses. Proc. Natl. Acad. Sci. U. S. A. 112, 6682–6687 [PubMed: 25964334]
49. Li N. et al. (2017) Immune-checkpoint protein VISTA critically regulates the IL-23/IL-17 inflammatory axis. Sci. Rep. 7, 1485 [PubMed: 28469254]
50. Xu W. et al. (2019) Immune-checkpoint protein vista regulates antitumor immunity by controlling myeloid cell-mediated inflammation and immunosuppression. Cancer Immunol. Res. 7, 1497–1510 [PubMed: 31340983]
51. ElTanbouly MA et al. (2020) VISTA re-programs macrophage biology through the combined regulation of tolerance and anti-inflammatory pathways. Front. Immunol. 11, 580187
52. Li K. and Tian H. (2019) Development of small-molecule immune checkpoint inhibitors of PD-1/PD-L1 as a new therapeutic strategy for tumour immunotherapy. J. Drug Target. 27, 244–256 [PubMed: 29448849]
53. Gabr MT and Gambhir SS (2020) Discovery and optimization of small-molecule ligands for V-domain Ig suppressor of T-cell activation (VISTA). J. Am. Chem. Soc. 142, 16194–16198
54. Snyder L. and Powers G. Janssen Pharmaceuticals NV. Anti-VISTA antibodies and fragments, WO 2015/097536 A2
55. Johnston RJ Five Prime Therapeutics Inc. Antibodies binding to VISTA at acidic pH, WO 2019/183040 A1
56. Molloy M. et al. Trustees of Dartmouth College and Immunext Inc. Anti-human VISTA antibodies and use thereof, WO 2017/ 181139 A2
57. Kraus M. and Wolf B. (1996) Implications of acidic tumor microenvironment for neoplastic growth and cancer treatment: a computer analysis. Tumor Biol. 17, 133–154
58. Brand A. et al. (2016) LDHA-associated lactic acid production blunts tumor immunosurveillance by T and NK cells. Cell Metab. 24, 657–671 [PubMed: 27641098]
59. Huber V. et al. (2017) Cancer acidity: an ultimate frontier of tumor immune escape and a novel target of immunomodulation. Semin. Cancer Biol. 43, 74–89 [PubMed: 28267587]
60. Liu Y. et al. (2020) Intracellular pH regulates cancer and stem cell behaviors: a protein dynamics perspective. Front. Oncol. 10, 1401 [PubMed: 32983969]
61. Wu H. et al. (2020) T-cells produce acidic niches in lymph nodes to suppress their own effector functions. Nat. Commun. 11, 4113 [PubMed: 32807791]
62. Barker H. et al. (2017) Role of carbonic anhydrases in skin wound healing. Exp. Mol. Med. 49, e334 [PubMed: 28524177]
63. Han SH et al. (2009) Acidic pH environments increase the expression of cathepsin B in osteoblasts: the significance of ER stress in bone physiology. Immunopharmacol. Immunotoxicol. 31, 428–431 [PubMed: 19242848]
64. Schreml S. et al. (2011) 2D luminescence imaging of pH in vivo. Proc. Natl. Acad. Sci. U. S. A. 108, 2432–2437 [PubMed: 21262842]
65. Dvorak HF (1986) Tumors: wounds that do not heal. Similarities between tumor stroma generation and wound healing. N. Engl. J. Med. 315, 1650–1659 [PubMed: 3537791]
66. Cabrita R. et al. (2020) Tertiary lymphoid structures improve immunotherapy and survival in melanoma. Nature 577, 561–565 [PubMed: 31942071]
67. Riley JL (2009) PD-1 signaling in primary T cells. Immunol. Rev. 229, 114–125 [PubMed: 19426218]
68. Zarbock A. et al. (2008) PSGL-1 engagement by E-selectin signals through Src kinase Fgr and ITAM adapters DAP12 and FcRγ to induce slow leukocyte rolling. J. Exp. Med. 205, 2339–2347 [PubMed: 18794338]
69. DeLano WL (2002) Pymol: an open-source molecular graphics tool. CCP4 Newsl. Protein Crystallogr. 40, 1–8
70. Ley K. and Kansas GS (2004) Selectins in T-cell recruitment to non-lymphoid tissues and sites of inflammation. Nat. Rev. Immunol. 4, 325–335 [PubMed: 15122198]

71. Guan B. et al. (2014) Amiloride and guggulsterone suppression of esophageal cancer cell growth in vitro and in nude mouse xenografts. Front. Biol. (Beijing) 9, 75–81 [PubMed: 24999355]
72. Larsen AM et al. (2012) Gram-scale solution-phase synthesis of selective sodium bicarbonate co-transport inhibitor S0859: in vitro efficacy studies in breast cancer cells. ChemMedChem 7, 1808–1814 [PubMed: 22927258]
73. Wei R. et al. (2018) Suppressing glucose metabolism with epigallocatechin-3-gallate (EGCG) reduces breast cancer cell growth in preclinical models. Food Funct. 9, 5682–5696 [PubMed: 30310905]
74. Jiang L. et al. (2015) Targeting FoxM1 by thiostrepton inhibits growth and induces apoptosis of laryngeal squamous cell carcinoma. J. Cancer Res. Clin. Oncol. 141, 971–981 [PubMed: 25391371]
75. Kennedy KM and Dewhirst MW (2010) Tumor metabolism of lactate: the influence and therapeutic potential for MCT and CD147 regulation. Future Oncol. 6, 127–148 [PubMed: 20021214]
76. Ames S. et al. (2020) CAIX forms a transport metabolon with monocarboxylate transporters in human breast cancer cells. Oncogene 39, 1710–1723 [PubMed: 31723238]
77. Steffan JJ et al. (2009) Na^+/H^+ exchangers and RhoA regulate acidic extracellular pH-induced lysosome trafficking in prostate cancer cells. Traffic 10, 737–753 [PubMed: 19302267]
78. Giusti I. et al. (2008) Cathepsin B mediates the pH-dependent proinvasive activity of tumor-shed microvesicles. Neoplasia 10, 481–488 [PubMed: 18472965]
79. Vaupel P. et al. (2019) The Warburg effect: essential part of metabolic reprogramming and central contributor to cancer progression. Int. J. Radiat. Biol. 95, 912–919 [PubMed: 30822194]
80. Cui J. et al. (2014) FOXM1 promotes the Warburg effect and pancreatic cancer progression via transactivation of LDHA expression. Clin. Cancer Res. 20, 2595–2606 [PubMed: 24634381]
81. Osada-Oka M. et al. (2010) Glucose is necessary for stabilization of hypoxia-inducible factor-1α under hypoxia: contribution of the pentose phosphate pathway to this stabilization. FEBS Lett. 584, 3073–3079 [PubMed: 20621833]
82. Demidenko ZN and Blagosklonny MV (2011) The purpose of the HIF-1/PHD feedback loop: to limit mTOR-induced HIF-1α. Cell Cycle 10, 1557–1562 [PubMed: 21521942]
83. Mekhail K. et al. (2004) HIF activation by pH-dependent nucleolar sequestration of VHL. Nat. Cell Biol. 6, 642–647 [PubMed: 15181450]
84. Muz B. et al. (2015) The role of hypoxia in cancer progression, angiogenesis, metastasis, and resistance to therapy. Hypoxia 3, 83–92 [PubMed: 27774485]
85. Du J. et al. (2011) PI3K and ERK-induced Rac1 activation mediates hypoxia-induced HIF-1α expression in MCF-7 breast cancer cells. PLoS One 6, e25213
86. McDonald PC et al. (2016) Overcoming hypoxia-mediated tumor progression: combinatorial approaches targeting pH regulation, angiogenesis and immune dysfunction. Front. Cell Dev. Biol. 4, 27 [PubMed: 27066484]
87. Chiche J. et al. (2009) Hypoxia-inducible carbonic anhydrase IX and XII promote tumor cell growth by counteracting acidosis through the regulation of the intracellular pH. Cancer Res. 69, 358–368 [PubMed: 19118021]
88. Le Floch R. et al. (2011) CD147 subunit of lactate/H^+ symporters MCT1 and hypoxia-inducible MCT4 is critical for energetics and growth of glycolytic tumors. Proc. Natl. Acad. Sci. U. S. A. 108, 16663–16668
89. Damgaci S. et al. (2018) Hypoxia and acidosis: immune suppressors and therapeutic targets. Immunology 154, 354–362 [PubMed: 29485185]
90. Hu Y. et al. (2012) K-ras G12V transformation leads to mitochondrial dysfunction and a metabolic switch from oxidative phosphorylation to glycolysis. Cell Res. 22, 399–412 [PubMed: 21876558]
91. Rathmell JC et al. (2003) Akt-directed glucose metabolism can prevent bax conformation change and promote growth factor-independent survival. Mol. Cell. Biol. 23, 7315–7328 [PubMed: 14517300]
92. Gordan JD et al. (2007) HIF and c-Myc: sibling rivals for control of cancer cell metabolism and proliferation. Cancer Cell 12, 108–113 [PubMed: 17692803]

93. Matoba S. et al. (2006) p53 regulates mitochondrial respiration. Science 312, 1650–1653 [PubMed: 16728594]

Box 1.

Direct $H^+/HCO3^-$ Transporters That Regulate the Acidity of the Tumor Microenvironment

Monocarboxylate transporters (MCTs) are the predominant transporter that regulates pH by transporting lactate from the tumor cell [75]. MCT1 is constitutively expressed in almost all tissues, whereas other MCT family members show tissue-specific expression [75]. MCT4 is induced by hypoxia and is expressed on tumor cells. In association with carbonic anhydrase (CA) IX, MCT4 transports lactate and H^+ ions into the TME, thereby inducing an acidic extracellular pH (pHe) [75,76].

Na^+/H^+ exchanger 1 (NHE1) is a transmembrane protein that extrudes protons in conjunction with Na^+ uptake to maintain the alkaline intracellular pH (pHi). Through the phosphoinositide 3-kinase (PI3K) pathway and GTPase Ras-homologous (Rho), NHE1 leads to lysosomal exocytosis in response to acidic pHe [77]. Cathepsin B can be released in parallel and cleaves the inactive proprotein forms of matrix metallopeptidase (MMP)-9 and MMP-2, thereby activating them to degrade tumor extracellular matrix (ECM) [78]. This results in metastasis leading to a positive feedback loop of acidic pHe leading to increased tumor volume [77,78].

The $Na^+/HCO3^-$ transport channel (NBC) is distributed uniformly on the plasma membrane and associates with CA IX/II [60]. CAII associated with the NBC channel mediates the reverse hydration of CO_2, which is further hydrated by CAIX, leading to release of H^+ and HCO_3^- ions into the TME [26]. The HCO_3^- outside the cell is transported into the cell by NBC, resulting in increased pHi (>7.5) in cancer cells compared with normal cells (~7.4), whereas the H^+ remains outside the cell to create an acidic pHe [60].

Vacuolar-H^+-ATPase (V-ATPase) is a major proton-extrusion system that is widely distributed on lysosomal and mitochondrial membranes in healthy cells [61]. The major role of V-ATPases inside the normal cell is to aid acid-dependent protease trafficking and to facilitate the maturation of proteases inside acidic lysosomes [61]. In cancer cells, the a3 isoform redirects V-ATPases to the cell membrane, thereby directing the efflux of acids and cathepsins into the TME [61].

Box 2.

How Hypoxia and Oncogenes Regulate the Acidity of the Tumor Microenvironment

Hypoxia inducible factor-1α (HIF-1α), a subunit of HIF-1, is activated by hypoxia, leading to upregulation of multiple genes that lead to an acidic pHe in the TME [84]. HIF-1α induces vascular endothelial growth factor (VEGF) signaling that promotes angiogenesis [85]. Tumor angiogenesis leads to the rapid formation of leaky blood vessels that have increased interstitial pressure, poor perfusion, and accumulation of acidic metabolites [86]. In hypoxic tumor regions, HIF-1α activity diverts the oxygen from mitochondria and directs glycolytic metabolism and biomass production instead of cellular respiration, namely the Warburg effect. Simultaneously, HIF-1α induces the expression of glucose transporter 1 (GLUT1) that is essential for glucose uptake [84]. Glucose-6-phosphate dehydrogenase (G6PD) activity results in NADP production via another glucose pathway, the pentose-phosphate pathway (PPP), and this further stabilizes HIF-1α activity. The PPP is associated with the production of CO_2 that in turn generates H^+ ions through hydration catalyzed by CA IX/XII [81]. CA IX/XII mediate H^+ distribution via MCT1/MCT4 and CO_2 hydration via NBC channels, thereby promoting cytoplasmic alkalization and extracellular acidification, which facilitates tumor growth [87]. HIF-1α activity stimulates higher production of CD147, an MCT subunit that facilitates the proper disposition of MCT channel proteins in the plasma membrane [88]. Accumulation of lactate in the TME through MCT channels causes an acidic pHe [89]. Mammalian target of rapamycin (mTOR) helps HIF-1α protein stabilization. mTOR signaling is stimulated by the tumor-suppressor serine/threonine kinase LKB1 under nutritional stress [86].

Several oncogenic regulators drive the Warburg effect in the TME in addition to hypoxia. (i) The $KIRAS^{G12V}$ oncogene downregulates mitochondrial respiratory chain complex I and induces reactive oxygen species (ROS) generation, further resulting in mitochondrial dysfunction [90]. Protein kinase B (Akt) is activated as a result of mitochondrial dysfunction, thereby upregulating glucose metabolism [91]. (ii) c-Myc upregulates the expression of several genes involved in glucose metabolism, such as glucose transporter 1 (*SLC2A1*), pyruvate kinase (*PKM*), and lactate dehydrogenase A (*LDHA*) [92]. (iii) p53 mutations can disrupt the expression of SCO2 (synthesis of cytochrome *c* oxidase) which is essential for cytochrome *c* oxidase (COX) regulation, thereby upregulating the glycolysis pathway in a manner resembling a toggle-switch [93]. (iv) Forkhead box protein M1 (FOXM1) directly regulates the expression of *LDHA* by binding to its promoter, further inducing the production of lactate [80].

Highlights

V-domain Ig suppressor of T cell activation (VISTA) binds to V-set and Ig domain-containing 3 (VSIG3) and P-selectin glycoprotein ligand 1 (PSGL-1) ligands, and signaling may be bidirectional.

VISTA binds to PSGL-1 at acidic pH, such as in the tumor microenvironment (TME), but not at physiological pH.

VISTA activity imposes quiescence on mammalian myeloid and naïve T cells, and inhibits T cell activation and cytokine production. It can promote peripheral tolerance via enhanced activation-induced T cell death.

VISTA is particularly upregulated on myeloid-derived suppressor cells (MDSCs) via hypoxia, and can contribute to the immunoinhibitory functions of myeloid cells by reducing Toll-like receptor (TLR) signaling and cell migration, as well as by reprogramming myeloid cells towards reduced production of the proinflammatory cytokines interleukin (IL)-6, tumor necrosis factor (TNF)-α, and IL-12, and increased production of IL-10 and other anti-inflammatory mediators.

Antagonistic VISTA antibodies are in clinical development for treating some cancers; drugs that target the acidity of the TME might reduce immunoinhibitory activity in acidic niches and combine well with VISTA or checkpoint blockade therapies.

Outstanding Questions

In which situations and cell types are the interactions of VISTA with PSGL-1 and VSIG3 dominant? PSGL-1 is expressed on many hematopoietic cells, but VSIG3 on few, raising doubt about the activity of VSIG3 in immune cell interactions. Whether VSIG3 is the major interaction partner at physiological pH and PSGL-1 at acidic pH needs to be experimentally tested.

What are the downstream signaling pathways of VISTA, PSGL-1, and VSIG3? Understanding the molecules involved in transducing these signals will be beneficial for understanding the regulated events and for devising optimal interventions.

What other negatively charged ligands may potentially bind to the VISTA histidine-rich region to block or mediate signaling? The interaction with PSGL-1 is heavily dependent on charge–charge interactions, and other highly negatively charged molecules might have potential to interact with VISTA at low pH.

When are other checkpoint receptors (PD-1, TIM-3, LAG-3, CTLA-4, TIGIT) coexpressed with active PSGL-1 on activated and exhausted T lymphocytes? VISTA expression decreases in activated T cells, whereas most other exhaustion receptors increase. When do expression and signaling overlap?

What are the other scenarios, in addition to tumors, where acidic niches are created and which can potentiate VISTA immunoinhibitory activity? Because pH emerges as an important factor in regulating immune responses and VISTA activity, it is important to identify the various physiological processes that create acidic niches.

Would druggable pH modifiers augment the benefit of VISTA- or checkpoint-blockade cancer immunotherapy? The acidic pH dependency of VISTA interactions suggests that targeting pH might be a new way to reduce VISTA activity. Is targeting pH an alternative to VISTA blockade, or is it additive?

Do better therapeutic VISTA mAbs have an active or silent Fc? The majority of antagonistic anti-VISTA mAbs under development have an active Fc and may deplete myeloid cells. Is this therapeutically more effective or is blockade alone preferred?

Does mouse VISTA bind to mouse PSGL-1 in the same fashion as described for humans? Human VISTA has been shown to interact with mouse PSGL-1 in the human VISTA knock-in mouse, but mouse VISTA has not been shown to interact with mouse PSGL-1. Mouse and human PSGL-1 have two or three tyrosines, respectively, that are available for sulfation in the putative interaction region.

Why was the first VISTA mAb clinical trial halted, and was there an associated toxicity? The wide expression of VISTA in the hematopoietic compartment and brain microglia may create potential obstacles when targeting VISTA in clinical settings.

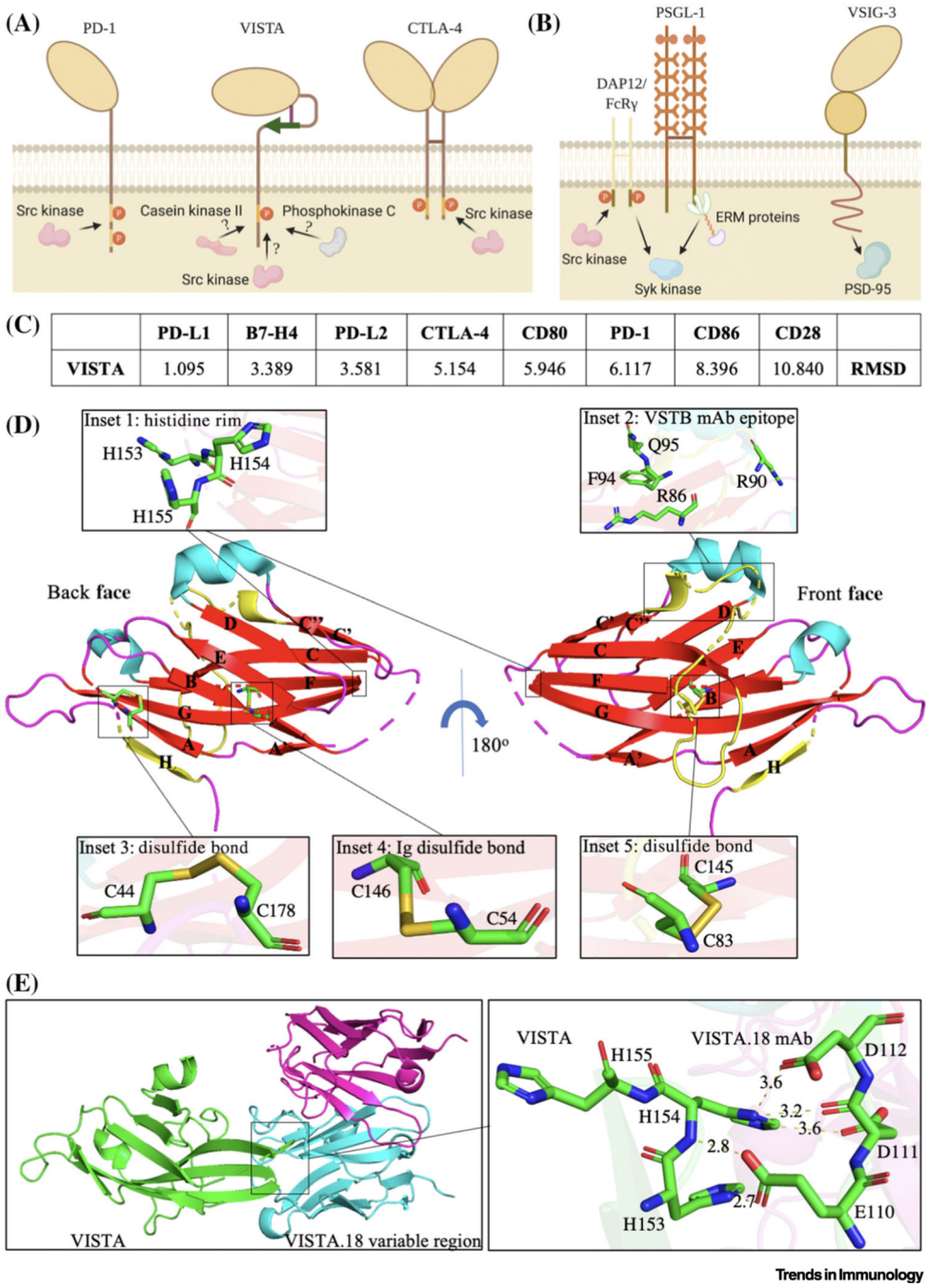

	PD-L1	B7-H4	PD-L2	CTLA-4	CD80	PD-1	CD86	CD28	
VISTA	1.095	3.389	3.581	5.154	5.946	6.117	8.396	10.840	**RMSD**

Figure 1. Structure of Human V-Domain Ig Suppressor of T Cell Activation (VISTA) and Its Ligands.

(A) VISTA contains a ‘clamped’ stalk region of nine amino acids, in contrast to the longer stalk of programmed cell death protein 1 (PD-1) (~20 amino acids) [29]. The PD-1 cytoplasmic domain contains an immunoreceptor tyrosine-based inhibitory motif (ITIM) (V/I/LxYxxL) and an immunoreceptor tyrosine-based switch motif (ITSM) (TxYxxL); cytotoxic T lymphocyte-associated protein 4 (CTLA-4) contains one SH2- (YxxM) and one SH3-binding (PxxP) motif [67]. The cytoplasmic domain of VISTA does not contain any immunoreceptor tyrosine-based signaling motifs [10]. However, it does have a conserved

SH2-binding motif (YxxQ) in the middle of the cytoplasmic tail, but it remains to be tested which motifs/kinases are important for signaling [9]. (B) P-selectin glycoprotein ligand 1 (PSGL-1) is a homodimeric 240 kDa adhesion molecule that mediates leukocyte trafficking by binding to selectins, which involves adaptor proteins DNAX-activating protein of 12 kDa (DAP12) and Fc receptor γ (FcRγ), ezrin, radixin, and moesin (ERM) proteins, and Src and Syk kinases [68]. The V-set and Ig domain-containing 3 (VSIG3) extracellular domain (ECD) contains an N-terminal IgV-like domain and an IgC-like domain. VSIG3 can function as an adhesion molecule that regulates synaptic transmission and plasticity by binding to postsynaptic scaffolding protein PSD-95 [12]. (C) Summary of root mean square deviation (RMSD) of superimpositions of VISTA (PDB 6U6V) and other B7 family members shows that VISTA most closely resembles PD-L1. (D) The ECD of VISTA (PDB 6U6V) generated with Pymol (C–C′ loop and H strand, yellow). Inset 1, histidine rim; inset 2, VSTB mAb epitope; inset 3, disulfide bond joining strands A and H; inset 4, Ig disulfide bond; inset 5, disulfide bond joining the C–C′ loop to the F strand. (E) Epitope targeted by pH-selective VISTA.18 monoclonal antibody (mAb) (PDB 6MVL). Putative hydrogen bonds calculated by Pymol [69]. Numbering of all amino acid positions is from Met = 1.

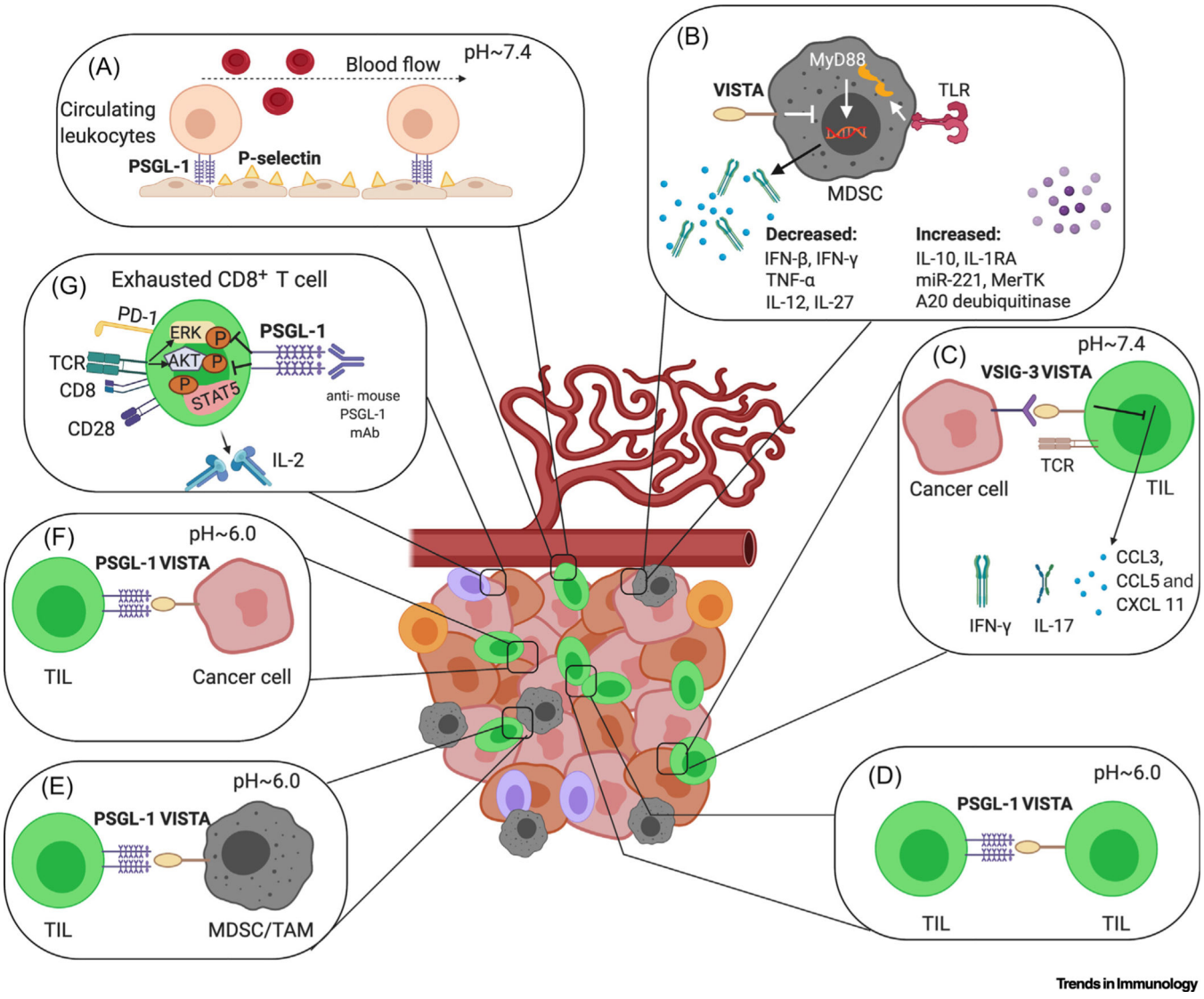

Figure 2. The Complexities of V-Domain Ig Suppressor of T Cell Activation (VISTA) Interactions.

In humans and mice, VISTA is highly expressed in the myeloid compartment, particularly in myeloid-derived suppressor cells (MDSCs), and in low amounts on tumor-infiltrating lymphocytes (TILs) [9]. VISTA can be expressed on cancer cells, although this is less common [33]. (A) Appropriately glycosylated and tyrosine sulfated P-selectin glycoprotein ligand 1 (PSGL-1) expressed on leukocytes binds to P-selectin molecules on the endothelium at physiological pH to facilitate leukocyte extravasation [70]. (B) In mice, VISTA signaling on myeloid cells can inhibit myeloid differentiation primary response 88 (MyD88)-dependent Toll-like receptor (TLR) signaling and cytokine production, and thereby induce a more immunosuppressive phenotype [50]. VISTA activity decreases proinflammatory cytokines and increases anti-inflammatory cytokines and mediators [50,51]. (C) In humans, the V-set and Ig domain-containing 3 (VSIG3) interaction with VISTA on T cells suppresses T cell activation and proliferation. This interaction is functional at neutral pH and the affinity declines fourfold at pH 6.0 [4]. (D–F) VISTA

expressed on cancer cells, MDSCs, or tumor-associated macrophages (TAMs) can bind to PSGL-1 on T cells at acidic pH but not at neutral pH. The signaling pathways of VISTA and PSGL-1 after ligation at pH 6.0 remain uncharacterized. (G) In mice, PSGL-1 ligation with anti-mouse PSGL-1 (clone 4RA10) leads to inhibition of T cell receptor (TCR) signaling and cytokine production via reduced phospho-ERK (extracellular signal-regulated kinase), protein kinase B (AKT), and signal transducer and activator of transcription 5 (STAT5), thereby promoting T cell exhaustion [23]. Abbreviations: CCL3, chemokine (C-C motif) ligand 3; CCL5, chemokine (C-C motif) ligand 5; CXCL11, C-X-C motif chemokine 11; IFN, interferon; IL, interleukin; mAb, monoclonal antibody; PD-1, programmed cell death protein 1; TNF, tumor necrosis factor.

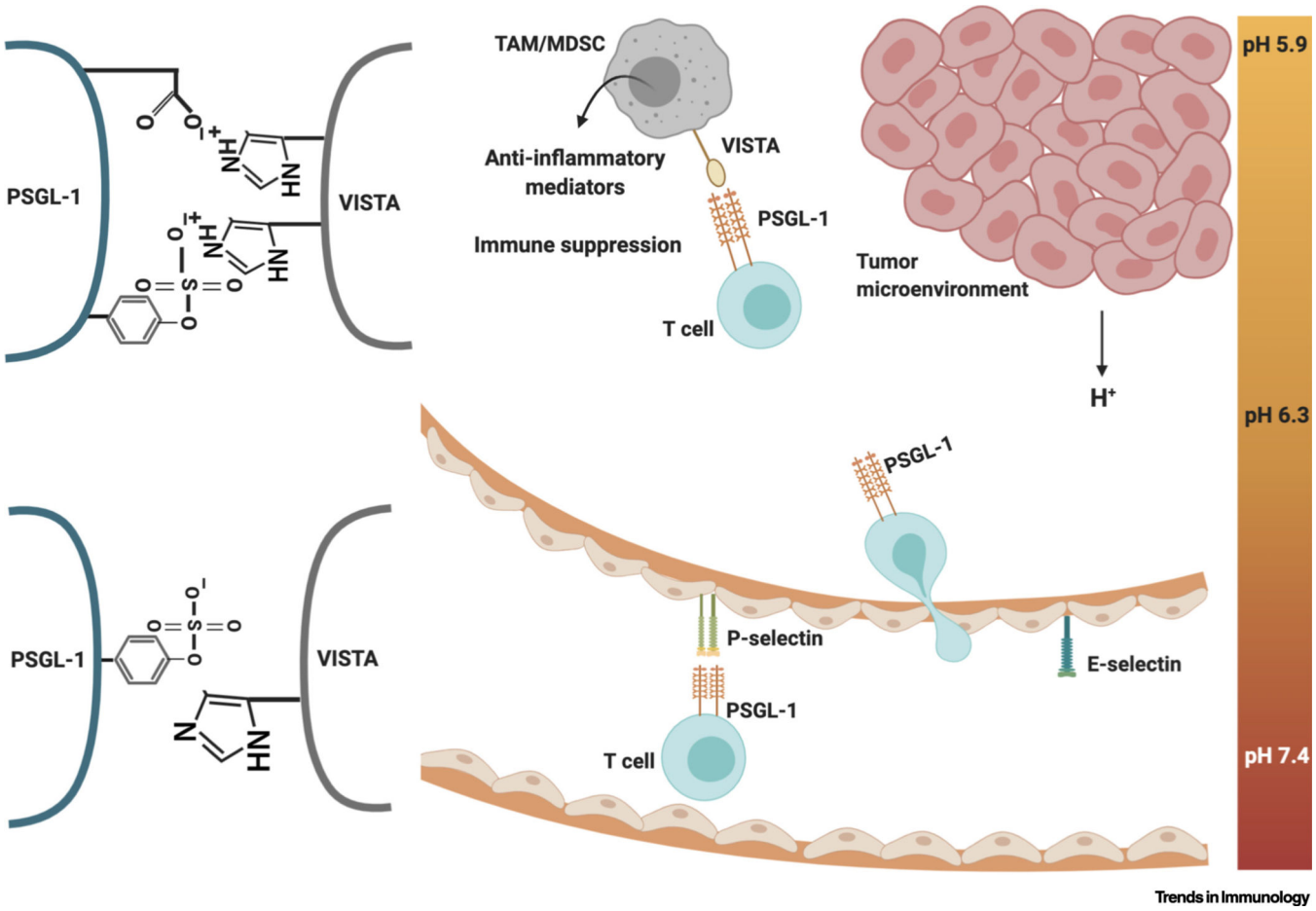

Figure 3. The Binding of Human V-Domain Ig Suppressor of T Cell Activation (VISTA) to P-selectin glycoprotein ligand 1 (PSGL-1) is pH-Dependent.

(Upper left) In acidic conditions, the VISTA histidines are protonated, allowing ionic interaction with negatively charged glutamic acid residues and sulfated tyrosines in PSGL-1 [3]. (Lower left) At pH 7.4, the histidine rim of VISTA is unprotonated and does not bind to PSGL-1. (Upper right) VISTA is highly expressed on myeloid-derived suppressor cells (MDSCs) and other myeloid cells. In the acidic tumor microenvironment (TME), PSGL-1 can interact with VISTA and mediate T cell and myeloid dysfunction. (Lower right) PSGL-1 is highly expressed on leukocytes such as T cells, and binding to selectins on endothelial cells at neutral pH mediates rolling of leukocytes along the vasculature and extravasation into tissues [3]. Abbreviation: TAM, tumor-associate macrophage.

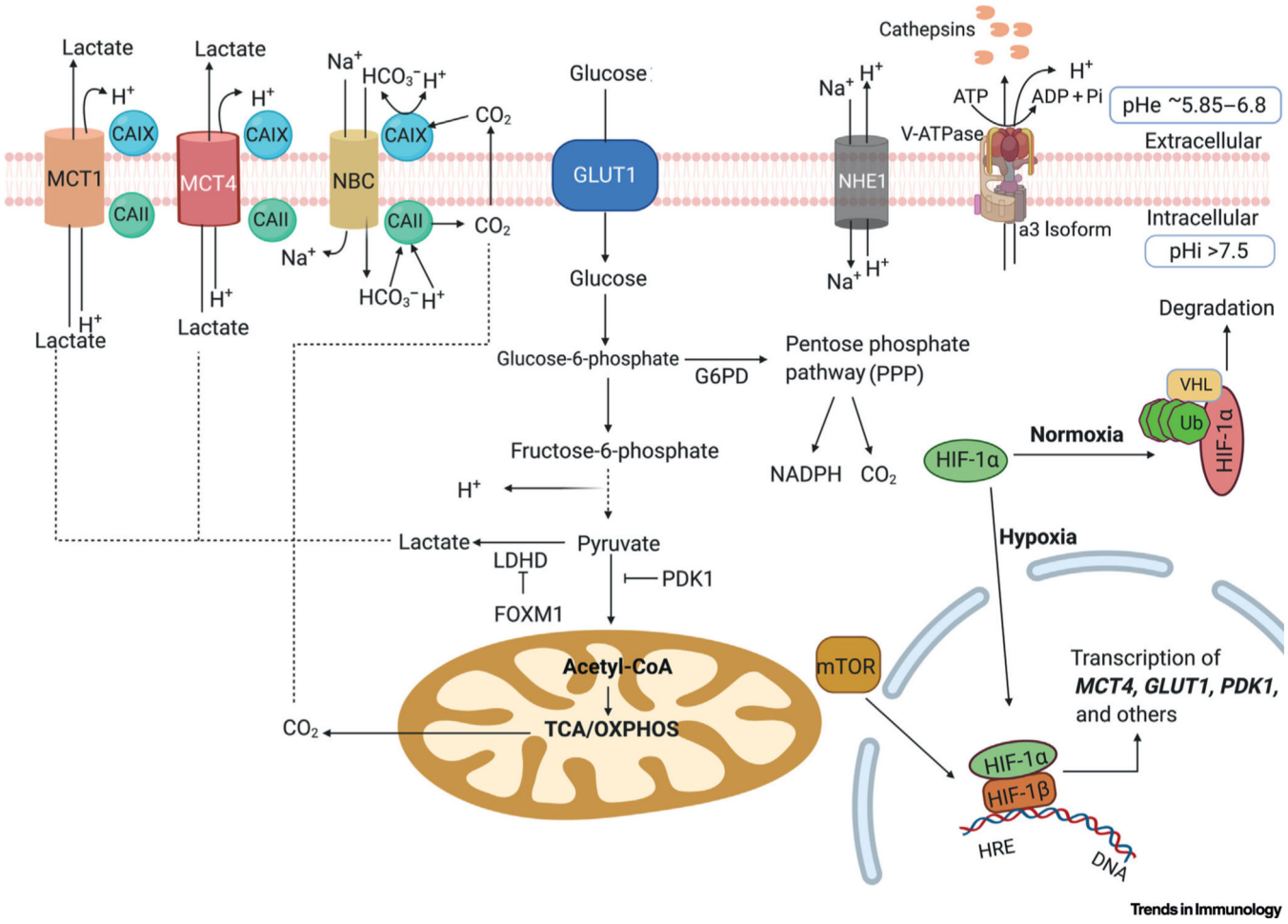

Figure 4. Mechanisms of pH Regulation in the Tumor Microenvironment (TME).

Monocarboxylate transporters 1 and 4 (MCT1/MCT4) mediate the efflux into the TME of lactate and H^+ generated by glycolysis [75]. Sodium bicarbonate transport channels (NBCs) maintain the alkaline intracellular pH (pHi) through the transport of HCO^-_3[26]. Carbonic anhydrases (CAIX/CAII) play a key role in two pathways (MCT and NBC), facilitating H^+ distribution and HCO^-_3 production, respectively [26]. Na^+/H^+ exchangers release H^+ into the TME through the influx of Na^+ [26]. Cancer cells express vacuolar-ATPase (V-ATPase) on the cell surface through utilization of the *a3* isoform, and this mediates the transport of cathepsins and H^+ from lysosomes to the TME [60]. In cancer cells, inhibition of cellular respiration by pyruvate dehydrogenase kinase (PDK) and increased activity of glucose transporter 1 (GLUT1), that transports glucose into the cell, promote glycolysis (the Warburg effect) [79]. Forkhead box protein M1 (FOXM1) binds to the promoter of the mitochondrial D-lactate dehydrogenase (*LDHD*) gene and enhances the expression of LDHD that converts pyruvate to lactate [80]. Glucose-6-phosphate generates CO_2 via glucose-6-phosphate dehydrogenase (G6PD) and the pentose-phosphate pathway (PPP) [81]. Mammalian target of rapamycin (mTOR) activation increases hypoxia-inducible factor (HIF)-1α translation [82]. During normoxia, HIF-1α binds to von Hippel–Lindau (VHL) and undergoes ubiquitination, resulting in proteasomal degradation of HIF-1 [83].

Abbreviations: HRE, hypoxia response element; OXPHOS, oxidative phosphorylation; pHe, extracellular pH; TCA, tricarboxylic acid cycle; Ub, ubiquitin.

Table 1.

pH Regulators in the TME: A Strategy To Reduce VISTA Immunoinhibitory Activity[a]

Target	Mechanism	Drug examples	Development in cancer treatment	Cancer type	Clinical trial accession number/Refs
MCT4	Transporter of lactic acid	Diclofenac	Phase I[b]	Solid tumors	NCT01596647[ii]
MCT1/2/4		AZD3965	Phase I	Solid tumors	NCT01791595[iii]
V-ATPases	Transporter of H^+/K^+	Omeprazole	Phase I–II[b]	Colorectal cancer (Phase II), solid tumors (Phase I), non-Hodgkin's lymphoma (Phase I)	NCT03086070[iv], NCT02518373[v], NCT00442741[vi], NCT00298779[vii],
NHE1	Na^+/H^+ exchanger	Amiloride	Preclinical[b]	Esophageal cancer	[71]
NBC	Na^+/HCO_3^- transporter	S3705	Preclinical	Breast cancer	[72]
LDHA	Warburg effect	Epigallocathehin	Preclinical	Breast cancer	[73]
FOXM1		Thiostrepton	Preclinical	Laryngeal squamous carcinoma	[74]
HIF2α/ HIF1α	Hypoxia-inducible factor	PT2977/MK-6482	Phase II	Kidney cancer	NCT03634540[viii]
		PT2385	Phase II	Glioblastoma	NCT03216499[ix]
		RO7070179	Phase I	Hepatocellular cancer	NCT02564614[x]
Hypoxia-regulated pathways/ targets	Carbonic anhydrase IX/XII	Tirapazamine (TPZ)	Phase I–III	Cervical cancer (Phase II), NSCLC (Phase III combinatorial), hepatocellular carcinoma (Phase I), gastrointestinal cancer (Phase II)	NCT00003369[xi], NCT00017459[xii], NCT02174549[xiii]
		Acetazolamide	Phase I	Small cell lung cancer (Phase I)	NCT03467360[xiv]
		Evofosfamide (TH-302)	Phase I	Advanced leukemia, solid tumors, esophageal cancer, pancreatic cancer, melanoma, squamous cell carcinoma of head and neck, prostate	NCT01833546[xv], NCT01149915[xvi], NCT02598687[xvii], NCT03098160[xviii]

[ii] https://clinicaltrials.gov/ct2/show/NCT01596647
[iii] https://clinicaltrials.gov/ct2/show/NCT01791595
[iv] https://clinicaltrials.gov/ct2/show/NCT03086070
[v] https://clinicaltrials.gov/ct2/show/NCT02518373
[vi] https://clinicaltrials.gov/ct2/show/NCT00442741
[vii] https://clinicaltrials.gov/ct2/show/NCT00298779
[viii] https://clinicaltrials.gov/ct2/show/NCT03634540
[ix] https://clinicaltrials.gov/ct2/show/NCT03216499
[x] https://clinicaltrials.gov/ct2/show/NCT02564614
[xi] https://clinicaltrials.gov/ct2/show/NCT00003369
[xii] https://clinicaltrials.gov/ct2/show/NCT00017459
[xiii] https://clinicaltrials.gov/ct2/show/NCT02174549

Target	Mechanism	Drug examples	Development in cancer treatment	Cancer type	Clinical trial accession number/Refs
				cancer (Phase I in combination with ipilimumab)	
	H^+	Sodium bicarbonate	Phase I	Malignant neoplasm	NCT02531919[xix]
	Reactive oxygen species	*N*-acetyl-L-cysteine	Phase I	Breast cancer	NCT01878695[xx]
	VEGF (angiogenesis)	Sunitinib, axinitib	FDA-approved	Kidney cancer, prostate cancer (Phase II), esophageal cancer (Phase II)	NCT0029974[xxi], NCT00702884[xxii], NCT00814021[xxiii]
		NVP-BEZ235	Phase Ib/II	Breast cancer	NCT01288092[xxiv]
	PI3K, ERK, mTOR signaling (mTORC1)	Everolimus (RAD001)	FDA-approved	Breast cancer, neuroendocrine cancer, kidney cancer (FDA-approved), gastric cancer (Phase I), pancreatic cancer (Phase II), NSCLC (Phase I), non-Hodgkin lymphoma (Phase I)	NCT01099527[xxv], NCT00409292[xxvi], NCT01700400[xxvii], NCT00622258[xxviii]
		Temsirolimus (CCI-779)	FDA-approved	Kidney cancer (FDA-approved), breast cancer (Phase II), glioblastoma (Phase II), mantle cell lymphoma (Phase III), prostate cancer (Phase II), bladder cancer (Phase II)	NCT02642094[xxix], NCT00016328[xxx], NCT00117598[xxxi], NCT0049409[xxxii], NCT00919035[xxxiii], NCT01827943[xxxiv]
		Rapamycin	Phase II[b]	Breast cancer (Phase II in combination with urastuzumab), prostate cancer (Phase I), bladder cancer	NCT00411788[xxxv], NCT03618355[xxxvi], NCT04375813[xxxvii], NCT00047073[xxxviii]

[xiv] https://clinicaltrials.gov/ct2/show/NCT03467360
[xv] https://clinicaltrials.gov/ct2/show/NCT01833546
[xvi] https://clinicaltrials.gov/ct2/show/NCT01149915
[xvii] https://clinicaltrials.gov/ct2/show/NCT02598687
xviii: https://clinicaltrials.gov/ct2/show/NCT03098160
[xix] https://clinicaltrials.gov/ct2/show/NCT02531919
[xx] https://clinicaltrials.gov/ct2/show/NCT01878695
[xxi] https://clinicaltrials.gov/ct2/show/NCT0029974
[xxii] https://clinicaltrials.gov/ct2/show/NCT00702884
xxiii: https://clinicaltrials.gov/ct2/show/NCT00814021
[xxiv] https://clinicaltrials.gov/ct2/show/NCT01288092
[xxv] https://clinicaltrials.gov/ct2/show/NCT01099527
[xxvi] https://clinicaltrials.gov/ct2/show/NCT00409292
xxvii: https://clinicaltrials.gov/ct2/show/NCT01700400
xxviii: https://clinicaltrials.gov/ct2/show/NCT00622258
[xxix] https://clinicaltrials.gov/ct2/show/NCT02642094
[xxx] https://clinicaltrials.gov/ct2/show/NCT00016328
[xxxi] https://clinicaltrials.gov/ct2/show/NCT00117598
xxxii: https://clinicaltrials.gov/ct2/show/NCT0049409
xxxiii: https://clinicaltrials.gov/ct2/show/NCT00919035

Target	Mechanism	Drug examples	Development in cancer treatment	Cancer type	Clinical trial accession number/Refs
				(Phase II), glioblastoma (Phase II)	
		AZD2014	Phase I	Prostate cancer (Phase I)	NCT02064608[xxxix]

[a] Abbreviations: CA, carbonic anhydrase; ERK, extracellular signal-regulated kinase; FOXM1, forkhead box protein M1; GLUT1, glucose transporter 1; HIF-1α, hypoxia-inducible factor 1α; LDHA, lactate dehydrogenase A; MCT, monocarboxylate transporter; mTOR, mammalian target of rapamycin; mTORC1, mammalian target of rapamycin complex I; NBC, Na^+/HCO_3^- transporter; NHE1, Na^+/H^+ exchanger 1; PI3K, phosphoinositide 3-kinase; ROS, reactive oxygen species; V-ATPase, vacuolar ATPase; VEGF, vascular endothelial growth factor.

[b] Medication with FDA approval in nonmalignant indications.

xxxiv: https://clinicaltrials.gov/ct2/show/NCT01827943
[xxxv] https://clinicaltrials.gov/ct2/show/NCT00411788
xxxvi: https://clinicaltrials.gov/ct2/show/NCT03618355
xxxvii: https://clinicaltrials.gov/ct2/show/NCT04375813
xxxviii: https://clinicaltrials.gov/ct2/show/NCT00047073
xxxix: https://clinicaltrials.gov/ct2/show/NCT02064608